Equatorial currents transport changes for extreme warm and cold events in the Atlantic Ocean

Marlos Góes and Ilana Wainer

Instituto Oceanográfico da Universidade de São Paulo, Departamento de Oceanografia Física, Brazil

Received 20 June 2002; accepted 20 November 2002; published 8 March 2003.

[1] In this work the Equatorial Atlantic Ocean circulation dynamics for warm and cold composite events are analyzed. Warm and cold typical years were composited from the respective five warmest and the five coldest years of the available record. Equatorial currents velocity and transport are calculated. During a typical warm event, the circulation decreases in the upper ocean, while during the typical cold event there is intensification. The strengthening (weakening) of the circulation during cold (warm) events increases (decreases) the stress between the Equatorial Undercurrent (EUC) and the South Equatorial Current (SEC), associated with an increase (decrease) in entrainment of cold waters into the surface and their westward transport. The EUC showed striking differences between both composited events. For the cold (warm) event the EUC shows a greater (reduced) transport and core velocity, and a deeper (shallower) structure. *INDEX TERMS:* 4231 Oceanography: General: Equatorial oceanography; 4572 Oceanography: Physical: Upper ocean processes; 4512 Currents; 4504 Air/sea interactions (0312). **Citation:** Góes, M., and I. Wainer, Equatorial currents transport changes for extreme warm and cold events in the Atlantic Ocean, *Geophys. Res. Lett.*, *30*(5), 8006, doi:10.1029/2002GL015707, 2003.

1. Introduction

[2] With respect to sea surface temperature (SST), the tropical Atlantic ocean displays two dominant modes of interanual variability largely described in the literature [e.g. *Servain*, 1991; *Wainer et al.*, 2002; *Servain et al.*, 2002]. One represents an inter-hemispheric SST gradient signature. The other is an equatorial mode, similar to the one associated to the Pacific Ocean El Niño - Southern Oscillation (ENSO) phenomena. This Atlantic "El Niño-like" mode is much weaker than its Pacific counterpart. They are similar in the fact that they relate the ocean's equatorial adjustment to sudden changes in the trade winds. With the intensification (weakening) of the winds in the western Atlantic the equatorial ocean responds with negative (positive) SST anomalies represented by cold and warm events. Equatorial Kelvin waves forced by the wind anomalies cause a perturbation of the zonal current field [*Siedel and Giese*, 1999]. Thus, as the EUC and SEC are the main equatorial currents responsible for the heat transport across the basin, they undergo significant changes during the extreme events and cause anomalous heat advection towards the eastern side of the basin. In this work, 40 years of simulation data from the National Center for Atmospheric Research -NCAR Ocean Model (NCOM) forced by NCEP monthly mean wind stress and fluxes are analyzed in order to understand changes in the equatorial current system from warm to cold phases.

0094-8276/03/2002GL015707$05.00

2. The Numerical Model

[3] The NCOM is an oceanic general circulation model [*Gent et al.*, 1998] that was forced with 40 years of NCEP-reanalysis winds (1958–1997) using the bulk scheme described in [*Large et al.*, 1997], with *non local "K profile parameterization"* (KPP) on vertical mixing [*Large et al.*, 1994] and [*Gent and McWilliams*, 1990] isopycnal mixing. This is a standard primitive equation model solved in spherical coordinates in an Arakawa B grid. The spatial resolution is 2.4° in longitude and is variable in latitude (1.2° at the equator trough 2.3° at medium latitudes). Forty-five vertical levels are used.

3. The Extreme Events

[4] In order to recognize the variability of the Atlantic equatorial mode we construct a SST index (Figure 1) based on the ATL3 index from *Zebiak* [1993], composed by the SST anomalies relative to the 1958–1997 model climatology, in the region bounded by 5°N–5°S/20°W–10°E. This ATL3 index was created taking into account the area of largest near-equatorial SST variability [*Carton and Huang*, 1994]. Superposed on this series is the time series for the same ATL3 index obtained from COADS-based observations [*Da Silva et al.*, 1994]. The correlation between the two series is approximately 0.8 with a 95 % confidence level.

[5] From this index the 5 warmest years and the 5 coldest years were selected, represented by the highest anomalies. The warmest years selected in this period were 1963, 1984, 1988, 1991 and 1995 and the coldest years selected were 1958, 1964, 1965, 1978 and 1983.

[6] Taking the mean of all warm events considered here, it is noted that they usually occur in July, suggesting a strong seasonal influence. The wind stress anomalies in the western equatorial region (50°W-25°W/5°S-5°N) which forces remotely the SST anomalies in the eastern side of the basin generally show their maximum one or two months before the maximum in the SST anomalies (figure not shown).

[7] Following the selection criterion (of years with maximum anomalies) described before, ocean velocities were also composited relative to warm and cold events which consisted of the monthly calendar average for the warmest and coldest years of the period, respectively [*Rasmusson and Carpenter*, 1982].

4. Transport changes for the EUC and SEC

[8] Figure 2 shows the averaged zonal transport for the EUC (Figure 2a) and SEC (Figure 2b) across the Atlantic basin for the model climatology (i.e. 40 years averaged annual cycle) and for warm and cold composited years. The

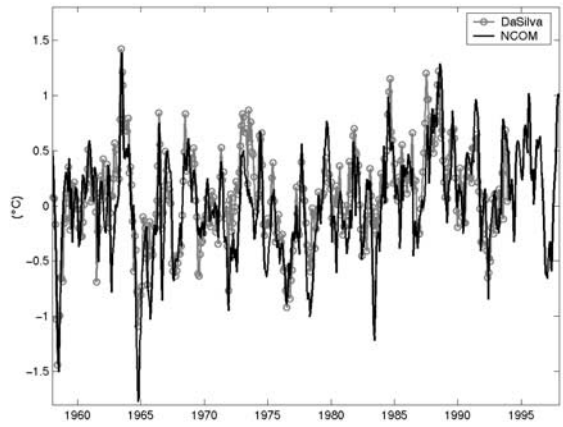

Figure 1. Time series of the SST index for NCOM simulation (black curve) and the observed DaSilva data set [*Da Silva et al.*, 1994] (gray curve with dots).

EUC transport was calculated using velocities greater than 20 cm/s. [*Katz et al.*, 1981; *Goriou and Reverdin*, 1992]. The SEC transport was calculated between 2.5°S and 2.5°N in the upper 50 meters only for westward velocities as *Philander and Pacanowski* [1986a]. It was calculated this way to represent the oceanic upper layer and because most of the SEC flow is located in this layer.

[9] The differences between the EUC transport (Figure 2a) for composited warm and cold years begin to increase at 33°W. The transport value for the composited warm year reaches its maximum of 4.2 Sv at 30°W. For the composited cold year the transport is 5.2 Sv at 30°W and increases to 5.9 Sv at 25°W. The maximum difference in transport between events occurs at 24°W of about 1.8 Sv. The SEC transport for the 3 cases (warm and cold composites and climatology) can be seen in Figure 2b. The smallest transport values are on the eastern side of the basin (2.3–3 Sv) and as the SEC flows westward these values increase until the maximum in the west (4.1–5.7 Sv). The highest differences between the composited warm and cold events are at approximately 31°W of about 2 Sv.

[10] Figure 3 shows the seasonal variations of the transports at 28°W for the EUC (Figure 3a) and the SEC. (Figure

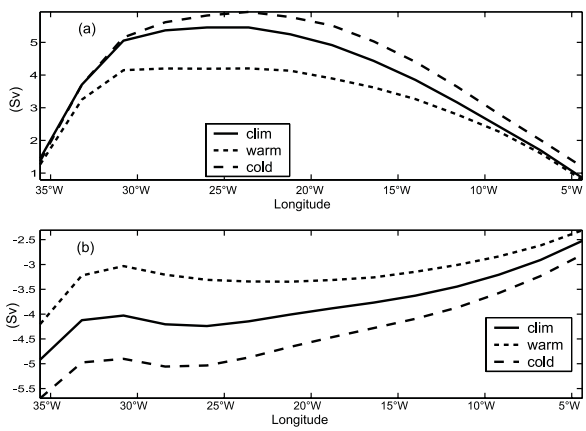

Figure 2. Annual mean zonal transport in Sv for (a) EUC and (b) SEC. Dashed curve: composited cold year. Dotted line: composited warm year. Black curve: climatology.

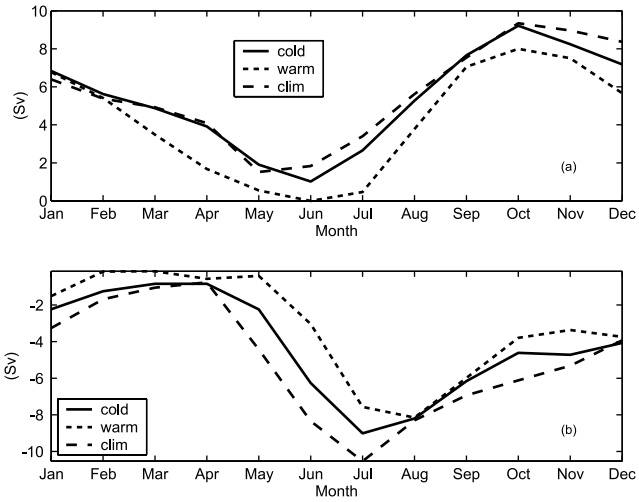

Figure 3. Transport (Sv) at 28°W for (a) EUC and (b) SEC. Dashed curve: composited cold year. Dotted line: composited warm year. Black curve: climatology.

3b). The EUC transport (Figure 3a) shows lower values from April to July and higher values starting from September [e.g. *Stramma and Schott*, 1996]. The SEC transport (Figure 3a) shows higher values from May to August [e.g. *Philander and Pacanowski*, 1986a]. It can be seen that the EUC and SEC transports are weaker during the composited warm year compared to the higher values obtained during the composited cold year. The highest differences between the events are of ~3 Sv in July for the EUC and ~5.5 Sv in May for the SEC.

[11] The EUC core velocity and depth for the composited warm and cold years and climatology is shown in Figure 4. A seasonal cycle is seen in the climatological EUC core velocity (Figure 4b), with smaller values from April through June with about 25 cm/s and the larger values on October and November with about 55 cm/s. The composited cold year shows maximum EUC velocity (57.8 cm/s) and a minimum core velocity (26.1 cm/s) larger than climatology while the composited warm year shows maximum EUC velocity

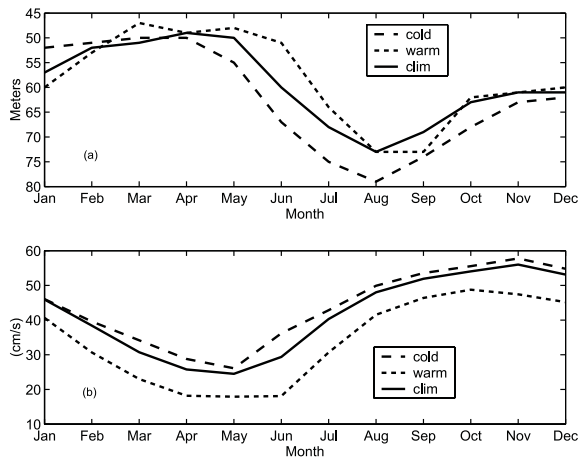

Figure 4. (a) EUC core depth (m) and (b) core velocity (cm/s). Dashed curve: composited cold year, Dotted line: composited warm year. Black curve: climatology.

(48.8 cm/s) and a minimum core velocity (17.9 cm/s) smaller than climatology for the whole year. These model velocities are weaker than observations. Furthermore, the observations don't show such a well defined seasonal cycle [*Weisberg et al.*, 1987]. However, the seasonal cycle of the EUC core depth (Figure 4a) is in agreement with [*Philander and Pacanowski*, 1986b], where it shows a minimum depth in April and a maximum depth in August–September. In April, when the EUC core is shallower (Figure 4a), the climatological core depth is ~49m and in August and September the climatological core is deeper (~73 m). The EUC core is generally between 50 m and 100 m as in [*Weisberg et al.*, 1987]. From April to August (Figure 4a), the EUC core for the warm year becomes shallower than the mean reaching a maximum difference of 9m in June. The depth of the EUC core for the composited cold year is deeper than the mean value throughout most of the year with maximum difference of 6 meters in August.

[12] It should be noted that according to the results of *Large et al.* [2001], the key element of this model is the spatially variable, anisotropic horizontal viscosity. It allows the coefficient of meridional diffusion of zonal momentum to be a physically based small value everywhere except near western boundaries. In the Atlantic equatorial basin however, it appears as if the viscosity remains too large, too far east of South America and the consequence is that the EUC never achieves an eastward velocity more than about half of that observed. The EUC maximum velocities in the observations may reach 120 cm/s, while in the NCOM these velocities are able to reach only 70 cm/s. Nonetheless, the model resolves all the main currents in the Atlantic Ocean, their seasonal variability and the interanual SST variability, which are agreement with observations and other model studies.

5. Mixed Layer

[13] The mixing processes at the equator are strongly influenced by the shears of the mean currents. This process can be quantified using the Richardson number (Ri), defined as the buoyancy frequency squared divided by the velocity shear squared. It's computed as $Ri = (\alpha g \partial T/\partial z)/[(\partial u/\partial z)^2 + (\partial v/\partial z)^2]$ where T, z, u and v are the respective temperature, depth, zonal and meridional velocities from the model, $g = 9.8\ m/s^2$ is the gravitational acceleration and $\alpha = 8.75 \times 10^{-6}\ (T + 9)\ °C^{-1}$ [*Hayes et al.*, 1991] is the coefficient of thermal expansion of water. Ri measures the competing effects of turbulence generation and stratification. The velocity shear acts to produce vertical mixing and the stratification acts to suppress mixing. This suggests that the vertical mixing is most intense above the core [*Weisberg and Wang*, 1997], between the EUC and the SEC, thus well correlated with the velocities from both currents. Besides the current shears, the temperature gradient influences the Ri. It's most intense in the thermocline, where the EUC core is located, and is well influenced by the surface heating and cooling. Therefore, Ri has a minimum above the core and a maximum at the core, as seen in July at 28°W (Figure 5a). The Ri values in the mixed layer are generally beneath the critical stable value ($Ri < 0.3$).

[14] Figure 5b shows $\tan^{-1}(Ri)$ at 28°W averaged over the mixed layer (defined here as the layer above 20°C). The upper ocean shear is related to the EUC core (Figure 4) and with the SST: as the core speed decreases the core rises and there is an associated increase in Ri. The warming of the surface contributes to increase the stratification which also increases the Ri. The highest Ri values ($Ri > 1.1$) are in the fall suggesting a decreasing in the shear, and the lowest values are from July to September ($0.8 > Ri > 0.5$), suggesting an intensification in the shear. Ri values are, as expected according to the Figures 3 and 4, smaller than the mean in the composited warm year and greater than the mean (from April on) for the composited cold year.

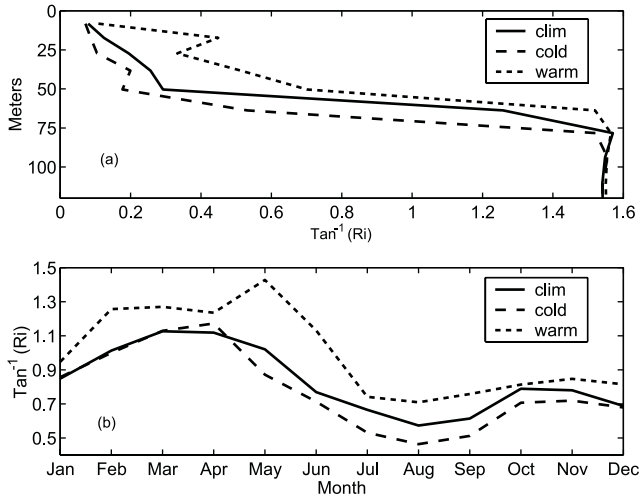

Figure 5. $Tan^{-1}(Ri)$ for averaged in the mixed layer. Dashed curve: composited cold year. Dotted line: composited warm year. Black curve: climatology. (a) as a function of depth and (b) as a function of time.

6. Conclusions

[15] In this work we used the oceanic component of the NCAR/CCSM model to describe the upper equatorial Atlantic circulation for extreme events years. Although the EUC never achieves an eastward velocity more than about half of that observed in the model, it resolves, nonetheless all the main currents in the Atlantic Ocean, their seasonal variability and the interanual SST variability, which are agreement with observations and other model studies.

[16] A typical warm and a typical cold year were constructed by the composite method. Both the EUC and the SEC transports increased for the composited cold year and diminished in the composited warm year relative to climatology. The annual EUC transport decreased from 1.8 Sv at 24°W between the composited warm and cold years and the maximum difference of 3 Sv occurred in July. For the SEC the major difference of 5.5 Sv between the composited warm and cold events occurred in May. The EUC core presented a shallower structure in the composited warm year with maximum difference from the climatology of 9m in June and a deeper structure in the composited cold year with a maximum difference of 6m in August. The core speed decreased during the composited warm year and increased during the composited cold year. In the mean the core speed was 2.3 cm/s higher in

the composited cold year and 7.1 cm/s lower in the composited warm year relative to climatology.

[17] As a variation in the speed and in the transport of the EUC and SEC is seen inside the mixed layer so is a variation in the velocity shear, quantified by the Richardson number (Ri) calculated relative to the model currents. The upper ocean shear is related to the EUC core. When the core velocity decreases it rises and there is an associated increase in Ri.

[18] In other words, during cold events, the overall Atlantic Ocean equatorial circulation strengthens: the EUC, which is responsible for the transport of cold waters from west to the east, has its maximum velocity and transport increased, while its core sinks. The also intensified SEC contributes to the increase of the upper layer mixing, which intensifies the entrainment of cold waters to the surface and their subsequent transport towards the center of the basin. The consequence is an overall cooling. During warm events, the reverse happens. The EUC velocity and transport weakens with an associated rise of its core. The SEC also weakens which decreases the upper layer mixing and accompanying the entrainment, leading to an overall warming.

[19] **Acknowledgments.** This work was supported in part by grants CNPq n° 300223/93-5, CNPq n° 453523/01-3, FAPESP n° 98/13397-400, FAPESP n° 99/07202-9 e FAPESP n° 00/2958-7. We wish to thank W. Large at NCAR for making the NCOM output available to us and to the SGER/NSF and NCAR for travel funds to I.W. NCAR is sponsored by the National Science Foundation.

References

Da Silva, A. M., C. C. Young, and S. Levitus, *Atlas of Surface Marine Data 1994*, vol. 1, *Algorithms and Procedures*, NOAA Atlas NESDIS 6, U.S. Department of Commerce, 83 pp., 1994.

Gent, P. R., and J. C. McWilliams, Isopycnal mixing in ocean circulation models, *J. Phys. Oceanogr.*, *20*, 150–155, 1990.

Gent, P. R., F. O. Bryan, G. Danabasoglu, S. C. Doney, W. R. Holland, W. G. Large, and J. C. McWilliams, The NCAR Climate System Model Global Ocean Component, *J. Climate*, *11*, 1287–1306, 1998.

Goriou, Y., and G. Reverdin, Isopycnal and diapycnal circulation of the upper equatorial Atlantic Ocean in 1983–1984, *J. Geophys. Res.*, *97*, 3543–3572, 1992.

Hayes, S. P., P. Cg, and M. J. Mcphaden, Variability of the sea surface temperature in the eastern equatorial Pacific during 1986–88, *J. Geophys. Res.*, *96*(C6), 10,533–10,566, 1991.

Katz, E. J., R. L. Molinari, D. E. Cartwright, P. Hisard, H. U. Lass, and A. de Mesquita, The seasonal transport of the equatorial Undercurrent in the western Atlantic (during the Global Weather Experiment), *Oceanol. Acta*, *4*(4), 445–450, 1981.

Large, W. G., J. C. McWilliams, and S. C. Doney, Oceanic vertical mixing: A review and a model with a nonlocal boundary layer parameterization, *Rev. Geophys.*, *32*, 363–403, 1994.

Large, W. G., G. Danabasoglu, S. C. Doney, and J. C. McWilliams, Sensitivity to surface forcing and boundary layer mixing in a global ocean model: Annual mean climatology, *J. Phys. Oceanogr.*, *27*, 2418–2447, 1997.

Philander, S. G. H., Unusual conditions in the tropical Atlantic Ocean in 1984, *Nature*, *322*, 236–238, 1986.

Philander, S. G. H., and R. C. Pacanowski, The Mass and Heat Budget in a Model of the Tropical Atlantic Ocean, *J. Geophys. Res.*, *91*(12), 14,212–14,220, 1986a.

Philander, S. G. H., and R. C. Pacanowski, A Model of the Seasonal Cycle in the Tropical Atlantic Ocean, *J. Geophys. Res.*, *91*, 14,192–14,206, 1986b.

Rasmusson, E. M., and T. H. Carpenter, Variations in Tropical Sea Surface Temperature and Surface Wind Fields Associated with the Southern Oscillation/El Niño, *Mon. Wea. Rev.*, *110*, 354–384, 1982.

Reverdin, G., P. Delécluse, C. Lévy, P. Andrich, A. Morlière, and J. M. Verstraete, The near surface tropical Atlantic in 1982–1984. Results from a numerical simulation and a data analysis, *Prog. Oceanogr.*, *27*, 273–340, 1991.

Servain, J., and M. Séva, On relationship between tropical Atlantic sea surface temperature, wind stress and regional precipitation indices: 1964–1984, *Ocean-Air Interactions*, *1*, 183–190, 1987.

Servain, J., Simple climatic indices for the tropical Atlantic Ocean and some applications, *J. Geophys. Res.*, *96*, 15,137–15,146, 1991.

Servain, J., G. Clauzet, and I. Wainer, Tropical Atlantic climate variability modes as observed from the PIRATA data set, *Geophys. Res. Letters*, (in press), 2002.

Wainer, I., G. Clauzet, and J. Servain, Time scales of upper ocean temperature variability inferred from the PIRATA data (1997–2000), *Submitted to Geophys. Res. Letters*, 2002.

Weisberg, R. H., J. H. Hickman, T. Y. Tang, and T. J. Weingartner, Velocity and temperature observations during the seasonal response of the Equatorial Atlantic Experiment at 0°, 28°W, *J. Geophys. Res.*, *92*, 5061–5075, 1987.

Weisberg, R. H., and C. Wang, Slow Variability in the Equatorial West-Central Pacific in Relation to ENSO, *J. Climate*, *10*, 1998–2017, 1997.

Zebiak, S., Air-sea interaction in the equatorial Atlantic region, *J. Climate*, *6*, 1567–1586, 1993.

M. Góes and I. Wainer, Instituto Oceanográfico da Universidade de São Paulo, Departamento de Oceanografia Física,Caixa Postal 66149, 05315-970 São Paulo, SP, Brasil. (wainer@usp.br; marlos@usp.br)